Metal-Ion-Dependent Catalysis and Specificity of CCA-Adding Enzymes: A Comparison of Two Classes[†]

Ya-Ming Hou,* Shan-Qing Gu, Haiping Zhou, and Lindsey Ingerman

Department of Biochemistry and Molecular Pharmacology, Thomas Jefferson University, 233 South 10th Street, Philadelphia, Pennsylvania 19107

Received May 21, 2005; Revised Manuscript Received July 20, 2005

ABSTRACT: The CCA-adding enzymes [ATP(CTP):tRNA nucleotidyl transferases] catalyze synthesis of the conserved and essential CCA sequence to the tRNA 3′ end. These enzymes are divided into two classes of distinct structures that differ in the overall orientation of the head to tail domains. However, the catalytic core of the two classes is conserved and contains three carboxylates in a geometry commonly found in DNA and RNA polymerases that use the two-metal-ion mechanism for phosphoryl transfer. Two important aspects of the two-metal-ion mechanism are tested here for CCA enzymes: the dependence on metal ions for catalysis and for specificity of nucleotide addition. Using the archaeal *Sulfolobus shibabae* enzyme as an example of the class I, and the bacterial *Escherichia coli* enzyme as an example of the class II, we show that both enzymes depend on metal ions for catalysis, and that both use primarily Mg^{2+} and Mn^{2+} as the "productive" metal ions, but several other metal ions such as Ca^{2+} as the "nonproductive" metal ions. Of the two productive metal ions, Mg^{2+} specifically promotes synthesis of the correct CCA, whereas Mn^{2+} preferentially accelerates synthesis of the noncognate CCC and poly(C). Thus, despite evolution of structural diversity of two classes, both classes use metal ions to determine catalysis and specificity. These results provide critical insights into the catalytic mechanism of CCA synthesis to allow the two classes to be related to each other, and to members of the larger family of DNA and RNA polymerases.

The tRNA CCA-adding enzymes catalyze the stepwise synthesis of the CCA sequence at the tRNA 3′ end (positions 74−76), which is required for amino acid attachment and interactions with the ribosome during protein synthesis, and for initiation of replication of retroviruses (*1*, *2*). The CCA enzymes[1] are universally present in all three primary domains of life (archaea, bacteria, and eukarya). They are unusual RNA polymerases because they synthesize the ordered CCA sequence without using a nucleic acid template, and thus are distinct from the template-dependent DNA and RNA polymerases. The CCA enzymes are also distinguished from poly(A) polymerase and terminal deoxytransferase, the two other nontemplated polymerases, by the precise nucleotide addition and termination. The catalytic mechanism of CCA enzymes has been a major interest for more than three decades.

Recent high-resolution X-ray crystal structures of two classes of CCA enzymes have stimulated further interest in their catalytic mechanism and specificity (*3*−*8*). Previous sequence alignment has divided these enzymes into two classes (*9*), where the archaeal enzymes belong to class I while the eukaryotic and eubacterial enzymes are class II. The two classes share little sequence homology, but can be both defined in crystal structures by four major domains (head, neck, body, and tail) of similar dimensions (*3*−*5*). Unexpectedly, the overall architectures of the two classes are entirely different. The class I structure consists of largely β strands and dimerizes through the body and tail domains of each monomer. This structure projects the head domain, which contains the catalytic core, at the far ends of the dimer structure (*4*, *5*). In contrast, the class II structure contains mostly α-helices and dimerizes through the head domain itself, projecting the tail outward (*3*). Importantly, of the four major domains, only the head domain is structurally homologous between the two classes. Each head domain features three conserved carboxylates (DXD and a third and more distant carboxylate) in a geometry similar to those of template-dependent DNA and RNA polymerases that use three carboxylates to coordinate two metal ions to catalyze phosphoryl transfer.

All known DNA and RNA polymerases are proposed to use the two-metal-ion mechanism for catalysis (*10*, *11*), including DNA polβ (*12*) and poly(A) polymerase (*13*) that are closely related to CCA enzymes. In the two-metal-ion mechanism of nucleotide addition, two divalent metal ions at ∼ 4 Å apart are bound to the phosphates of the incoming nucleotide and to the conserved carboxylates of the polymerase active site. One metal ion is positioned to lower the affinity of the 3′-OH of the extending primer for the hydrogen, enhancing the nucleophilicity of the 3′-O^- to attack on the α-phosphate of the incoming nucleotide. The other

[†] Supported by grants from NIH (GM068561) and American Cancer Society (PRG-99-347-01-GMC) to Y.-M.H. and a summer undergraduate fellowship from Jefferson Medical College to L.I.

* Corresponding author. Tel: 215-503-4480. Fax: 215-503-4954. E-mail: Ya-Ming.Hou@jefferson.edu.

[1] Abbreviations: CCA enzymes, CCA-adding enzymes, ATP(CTP): tRNA nucleotidyl transferases; *E. coli*, *Escherichia coli*; *S. shibatae*, *Sulfolobus shibatae*.

10.1021/bi0509402 CCC: $30.25
Published on Web 09/01/2005

metal ion is positioned to assist leaving of the pyrophosphate group. Both metal ions stabilize the structure and charge of the expected pentacovalent transition state to provide a simple mechanism for catalysis. This mechanism is also widely used by many nucleic acid metabolic enzymes, including site-specific restriction endonucleases, alkaline phosphatase, as well as ribozymes such as the self-splicing group I introns (*14*).

Although crystal structures suggest that both classes of CCA enzymes use the two-metal-ion mechanism for catalysis, no biochemical support for this mechanism exists, and many fundamental issues of the mechanism have not been established. As a first step to investigate the catalytic mechanism of CCA enzymes, two of the most important issues of the two-metal-ion mechanism are addressed here: the role of metal ions in catalysis of CCA addition, and the role of metal ions in the specificity of nucleotide incorporation. In the two-metal-ion mechanism, metal ions should directly determine catalysis, and additionally determine nucleotide selectivity by differentiating the rate of the cognate from that of the noncognate reaction. Several restriction enzymes, upon substitution of Mn^{2+} for Mg^{2+}, have markedly enhanced ability to catalyze noncognate reactions (*15*−*18*). Similarly, introduction of Mn^{2+} to DNA polymerases accelerates incorporation of noncognate base analogues (*19*).

Because of the overall major differences between the two classes of CCA enzymes, the ability to address the two fundamental issues raised above is particularly important for relating the two classes to each other, and to members of the larger family of all DNA and RNA polymerases. On the other hand, this will also provide an opportunity to identify features that are unique to each class of CCA enzymes. By studying the archaeal *Sulfolobus shibatae* CCA enzyme as an example of the class I, and the bacteria *Escherichia coli* CCA enzyme as an example of the class II, we have revealed differences and similarities between the two, which establish a functional basis to interpret their common catalytic core in diverse structures.

MATERIALS AND METHODS

CCA Enzymes and the RNA Substrate. The recombinant *E. coli* CCA enzyme with a C-terminal His-tag and the recombinant *S. shibatae* enzyme with an N-terminal His tag (a gift of Dr. AM Weiner, U. Washington) were expressed in *E. coli* BL21(DE3) and purified with the His-link metal affinity resin (Qiagen), followed by an FPLC Heparin chromatography. The purified enzymes were stored in 0.1 M glycine (pH 9.0), 10 mM DTT, and 40% glycerol at −20 °C. The RNA substrate Val-34C (Figure 1) was synthesized by Dharmacon and was purified by a denaturing 12% PAGE/7 M urea gel. It was 5′ labeled by T4 polynucleotide kinase (5 units, New England Biolabs) with [γ-^{32}P]ATP (3000 Ci/mmol, NEN) and gel purified and annealed before use.

Assays for Synthesis of CCA and Poly(C). Nucleotide addition to position 76 of Val-34C (1 μM) was assayed in 0.1 M glycine, pH 9.0, 1 mM divalent metal ion, 250 μM CTP and/or ATP (*20*). The *E. coli* enzyme was assayed at 0.03−0.1 μM at 37 °C while the *S. shibatae* enzyme was assayed at 3−10 μM at 60 °C in the same buffer condition. Aliquots of 3 μL were removed from an assay reaction at various time points and mixed with an equal volume of a denaturing dye containing 89 mM Tris-HCl, pH 8.1, 89 mM boric acid, 2 mM EDTA, 7 M urea, bromophenol blue (0.1%), and xylene cyanol (0.1%). The mixture (3 μL) was separated by electrophoresis on a denaturing 12% PAGE/7 M urea gel, and intensities of product (*p*) and substrate (*s*) were quantified by a phosphorimager (Molecular Dynamics). The velocity was calculated by determining the fraction of product conversion of the RNA substrate ($p/(p + s)$) per unit of time. The steady-state kinetic parameters of nucleotide addition were determined from the relationships between initial rates and concentrations of ATP or CTP, which were fit to the Michaelis−Menten equation to derive K_m and k_{cat}, using the KaleidaGraph software. Each K_m and k_{cat} was the average of at least 3 independent experiments.

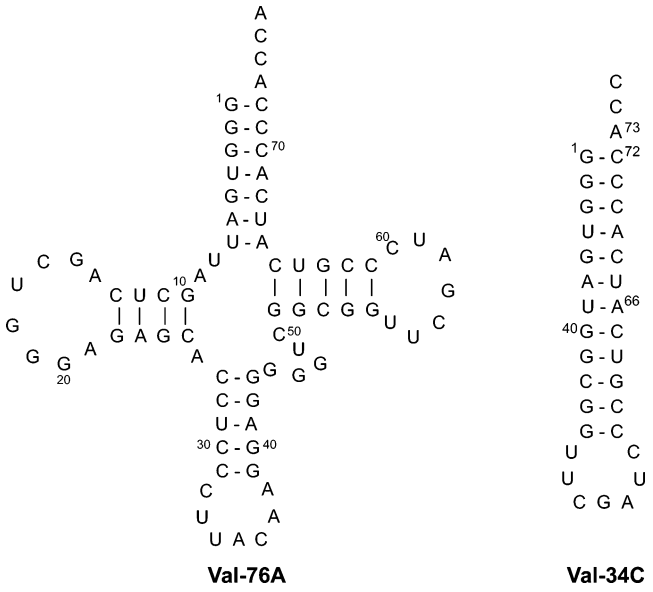

FIGURE 1: Sequences and secondary structures of (A) *E. coli* $tRNA^{Val}$ and (B) the Val-34C substrate for CCA enzymes. Numbering on the tRNA and minihelix is based on standard features of yeast $tRNA^{Phe}$.

Gel Shift Assay. Val-34C (^{32}P labeled) was incubated with varying concentrations of *S. shitabae* enzyme in the binding buffer (5 mM Hepes, pH 7.5, 25 mM KCl, 2 mM DTT, 3.8% glycerol) with or without 2 mM $MgCl_2$ at 37 °C for 10 min. The binding reaction (10 μL) was then mixed with a loading dye (3 μL) in the same binding buffer but with 0.01% xylene cyanole and bromophenol blue and 9% glycerol. The binding reaction was then loaded onto a 6.5% PAGE in 0.5 × TBE and 2.5% glycerol, electrophoresed in 0.5 × TBE for 1 h at 150 v (18 cm × 16 cm × 0.4 mm), room temperature. The gel was dried and analyzed by a phosphorimager.

Fluorescence Titration of Nucleotide Binding. All titration experiments were performed on the QM-4/2005 model spectro-fluorometer (Photon Technology International), using a high-intensity xenon source for excitation. Wavelength selection for excitation and emission was controlled by two computers through autocalibrated monochromators. The CCA enzyme (*E. coli* or *S. shibatae*) at 0.5 μM and saturated with Mg^{2+}, Mn^{2+}, or Ca^{2+} at 10 mM was titrated with increasing concentrations of ATP or CTP. The titration buffer for the *E. coli* enzyme was 20 mM Tris-HCl, pH 7.5, 2 mM DTT, while that for the *S. shibatae* enzyme was 100 mM glycine, pH 9.0. Excitation for both enzymes was at 285 nm, while

emission was monitored at 340 nm for the *E. coli* enzyme but at 335 nm for the *S. shibatae* enzyme. To correct for the inner filter effect of ATP and CTP absorption at the wavelength of excitation, a solution of tryptophan (0.5 μM) was titrated with 1 mM ATP or CTP to ensure that the emission of tryptophan was minimal, while that of CCA enzymes was significant. The titration curves of ATP binding or CTP binding to CCA enzymes were fit to the hyberbola equation to derive K_d values by KaleidaGraph analysis.

RESULTS

Metal Ions for Addition of A76 for Synthesis of the Cognate CCA Sequence. We focused on the nucleotide addition to position 76 of the CCA sequence as the primary assay for CCA enzymes. The rationale was based on our previous observations that, although both classes of CCA enzymes have an exclusive specificity for CTP for addition to positions 74 and 75, their specificity for addition to position 76 is subject to experimental conditions (*20*, *21*). For example, in the presence of both ATP and CTP, these enzymes overwhelmingly select ATP for addition to the CC end, whereas in the presence of only CTP, they synthesize CCC and poly(C), albeit with reduced catalytic rates compared to that of CCA (*21*). The synthesis of CCC and poly(C) can be effectively prevented by higher concentrations of ATP, such as 1 mM for the class I enzymes, and 0.1 mM for the class II enzymes (*21*). Under physiological conditions, where ATP is typically at 3−4 mM (*22*) and CTP at 0.05−0.2 mM (*23*), the CCA enzymes should synthesize only CCA. Although the synthesis of CCC and poly(C) is nonphysiological, this activity is useful for yielding insights into the catalytic mechanism. Similarly, many restriction enzymes catalyze cleavage at noncognate sites under nonphysiological conditions, such as low pH, low ionic strength, or organic solvents such as glycerol or DMSO (*15*). These noncognate reactions have revealed valuable information for understanding the specificity of restriction enzymes.

To test nucleotide addition to position 76, we used the Val-34C minihelix as the RNA substrate, which has 34 nucleotides in length and is terminated with C75 of the CC end (Figure 1). Val-34C consists of the acceptor−T stem−loop of *E. coli* $tRNA^{Val}$, which is the primary tRNA domain that is recognized by both classes in crystal structures (*7*, *8*), and is active for the stepwise nucleotide addition by both classes (*20*, *21*, *24*, *25*). Previous studies of addition to the 76 position of Val-34C were all performed with Mg^{2+}. Here, we tested the ability of the two classes of CCA enzymes to use different divalent metal ions for this addition (Figure 2A). If the catalytic mechanism depends on metal ions, we should observe different rates due to different preferences of divalent metal ions in coordinating inner-sphere ligands.

We chose the previously studied *S. shibatae* enzyme as a representative of the class I (*21*), and the *E. coli* enzyme as a representative of the class II (*20*). The two enzymes were both purified as a His-tagged recombinant form from *E. coli*, and were stored in a buffer without any metal ions. The addition of A76 to the CC end was monitored by electrophoresis on a denaturing PAGE/7 M urea gel, where the 34-mer Val-34C substrate was separated from the 35-mer product of Val-35A (Figure 2B,C). The Val-34C substrate was labeled with ^{32}P at the 5′ end, so that its conversion to

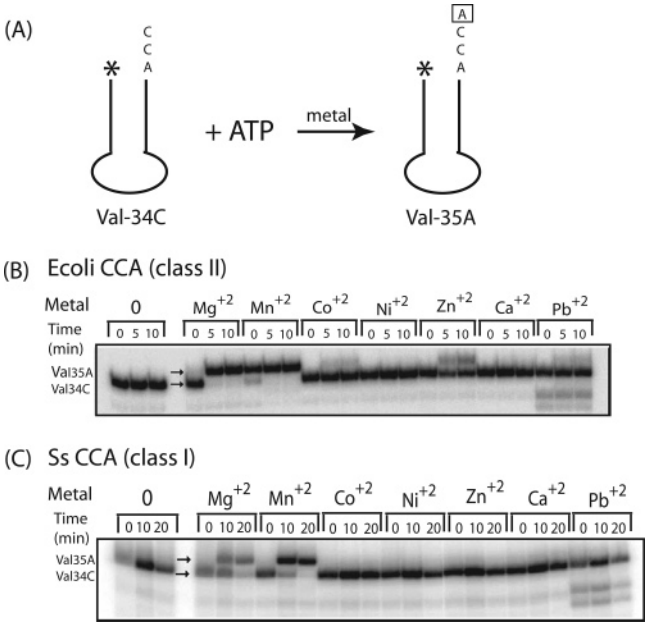

FIGURE 2: (A) Addition of ATP (250 μM) to Val-34C (1 μM, 5′ labeled with ^{32}P) catalyzed by a CCA enzyme in the presence of different divalent metal ions (1 mM each). (B) Addition catalyzed by the class II *E. coli* enzyme (0.02 μM for Mn^{2+} and Mg^{2+} reactions; 0.1 μM for Zn^{2+}, Co^{2+}, and Pb^{2+} reactions; 0.5 μM for Ni^{2+}, Ca^{2+} reactions). (C) Addition catalyzed by the class I *S. shibatae* enzyme (0.5 μM for Mn^{2+} and Mg^{2+} reactions, 30 μM for all other metal ions). The time course of the reactions is shown for each metal ion, and positions of the Val-34C substrate and Val-35A product are indicated by arrows.

product could be monitored by a phosphorimager analysis, and the rate of conversion could be determined by measuring the fraction of conversion per unit of time.

Several divalent metal ions, each at 1 mM, were tested for the addition of A76 to Val-34C by the *E. coli* enzyme (Figure 2B). The addition activity was assayed at pH 9.0, where all of the selected divalent metal ions were soluble at 1 mM. Certain metal ions at higher concentrations were prone to precipitate. Under the assay conditions, reactions of each metal ion were studied with a range of enzyme concentrations (0.02 to 0.5 μM) and time periods (1 min to 4 h) so that the initial reaction rates with each metal ion could be estimated. Because the concentration of the Val-34C substrate (1 μM) was significantly below the K_m of the RNA minihelix (263 μM) (*21*), the observed rates were approximately proportional to the k_{cat}/K_m parameter. By normalizing reaction rates against the enzyme and RNA concentrations, the k_{cat}/K_m values were obtained and compared for different metal ions. The relative activities decreased according to the order $Mn^{2+} > Mg^{2+} \gg Zn^{2+} = Co^{2+} \gg Ni^{2+} = Ca^{2+}$, where $>$ indicates a decrease of approximately 10-fold from the preceding cation, and $\gg$ indicates a decrease of more than 100-fold. Pb^{2+} was not included in the series, because although it promoted a weak activity (similar to that of Zn^{2+} and Co^{2+}), this metal ion also catalyzed cleavage of the RNA substrate. Importantly, while different divalent metal ions supported the nucleotide-addition activity to varying degrees, Mn^{2+} edged out Mg^{2+} with the highest activity. The Mn^{2+}-dependent activity was so strong under the assay condition (Figure 2B) that the product synthesis was evident at the time 0 point (within a fraction of a minute after enzyme addition). This comparison also revealed that Ni^{2+} and Ca^{2+} were nonproductive for

catalysis, with a rate reduced from that of Mn^{2+} by at least 10^5-10^6-fold.

The activity of the *S. shibatae* enzyme showed a more restricted range of metal ions and was supported by only Mg^{2+} and Mn^{2+} (1 mM each, Figure 2C). No other metal ions yielded any activities, even with elevated enzyme concentrations (to 50 μM). Despite this, the *S. shibatae* enzyme used the two active metal ions similarly as the *E. coli* enzyme. Mn^{2+} stimulated higher activity than Mg^{2+}, and was more efficient than Ca^{2+} by $\sim10^5-10^6$ fold. These experiments confirmed that the activity of the CCA enzymes, for both the *E. coli* and *S. shibatae*, is dependent on the type of metal ions used in the reaction. While Mn^{2+} and Mg^{2+} were the productive metal-ion cofactors, other metal ions such as Ca^{2+} were the nonproductive cofactors.

Metal Ions Are Required for Nucleotide Binding, but Not RNA-Binding. No activity of A76 addition was observed for the *E. coli* or *S. shibatae* enzyme when the reaction buffer contained no metal ions (Figure 2B,C). The lack of activity in the absence of metal ions was also observed in all of the experiments described below, which raised the possibility that metal ions were responsible for substrate binding and/or for catalysis. To test the role of metal ions in binding the nucleotide substrate, a fluorescence titration was developed, using intrinsic enzyme tryptophans as a probe. The *E. coli* enzyme contains 8 tryptophans, one of which (W24) is immediately on the C-terminal side of the catalytic DXD motif. The *S. shibatae* enzyme contains 7 tryptophans, one of which (W47) is prior to the DXD motif by 3 residues. Because it is not known which tryptophan was responsible for a fluorescence effect, the wild type of both enzymes was used for analysis. Three controls were performed to ensure that the fluorescence change was specific to nucleotide binding to the active site. First, titration of both enzymes with buffers at room temperature over a course of an hour showed no obvious photobleaching. Second, to correct the inner filter effect resulting from the absorption of excitation light by the addition of ATP or CTP, a solution of tryptophan was used as a control to titrate each nucleotide over a range of concentrations. This control was to identify an excitation wavelength to establish a fluorescence emission spectrum of the CCA enzymes that did not overlap with the spectrum of the free tryptophan solution. For both the *E. coli* and *S. shibatae* enzymes, a suitable condition was achieved by excitation at 285 nm and monitoring emission around 340 nm in an emission spectrum of 300−400 nm. In this condition, addition of ATP to these enzymes increased the fluorescence intensity, whereas addition of CTP quenched the intensity. Importantly, fluorescence titrations of both nucleotides were in a concentration-dependent manner that reached saturation at physiological nucleotide concentrations (see below). Third, the nonsubstrate GTP was used to confirm that the fluorescence change reflected specificity of nucleotide binding. In contrast to titration of ATP or CTP, addition of GTP to the *E. coli* CCA enzyme never reached saturation even up to 2 mM of the nucleotide (data not shown). The ability of the titration to discriminate against a nonsubstrate nucleotide suggested that the titration was specific, and that it most likely monitored nucleotide binding at the active site.

Titrations of ATP or CTP were performed in the presence of different metal ions at 10 mM each. These titrations did not include the RNA substrate, so that the binding of nucleotides to CCA enzymes can be interpreted directly, without the concern of RNA induced effect on nucleotide binding. Such an effect had been implicated by crystal structures of both classes of CCA enzymes (*7*, *8*). Mg^{2+} and Mn^{2+} were chosen as the productive metal ions, and Ca^{2+} was chosen as the nonproductive metal ion. All of these titrations displayed saturation curves (Figure 3), which could be fit to a hyperbolic equation to derive K_d values (Table 1). Most importantly, in all cases, titration of nucleotides without any metal ions revealed no change of fluorescence, indicating that the observed fluorescence change upon binding ATP or CTP was dependent on metal ions. However, as shown below, both productive and nonproductive metal ions contributed similarly to the binding.

For the *E. coli* enzyme with Mg^{2+} as the cofactor, titration of ATP yielded a K_d of 1.8 μM, which was similar to the previously determined K_d of 6.2 μM for the *E. coli* enzyme by a gel filtration assay (*26*). Replacement of Mg^{2+} with Mn^{2+} or Ca^{2+} reduced the amplitude of saturation (Figure 3A) but still yielded a K_d for ATP (4.7 and 4.6 μM, respectively, Table 1) only 2−3-fold higher than that in the presence of Mg^{2+} (Table 1). Similarly, titration of the Mg^{2+}-saturated *E. coli* enzyme with CTP revealed a K_d of 150 μM, which was in good agreement with the previously reported K_d of 188 μM by the gel filtration assay (*26*). This K_d changed little when Mg^{2+} was replaced by Mn^{2+} (K_d = 130 μM), or by Ca^{2+} (K_d = 180 μM) (Figure 3B, Table 1). The same trend was observed for the *S. shibatae* enzyme. Titration of ATP in the presence of Mg^{2+}, Mn^{2+}, and Ca^{2+} each yielded a K_d similar to each other (3.5, 2.5, and 2.5 μM, respectively, Figure 3C, Table 1). Conversely, titration of CTP in the presence of Mg^{2+}, Mn^{2+}, and Ca^{2+} also yielded a K_d within 2-fold of each other (230, 160, 130 μM, respectively, Figure 3D, Table 1). Thus, although Ca^{2+} is the nonproductive metal ion and Mg^{2+} and Mn^{2+} are the productive metal ions, all three metal ions elicited similar enzyme affinities to ATP and CTP, suggesting that the identity of metal ions was not important.

To examine the role of metal ions in binding the RNA substrate to CCA enzymes, a gel shift assay was developed. Previous studies have established that the class I *S. shibatae* enzyme showed a gel shift activity toward the tRNA substrate, but that the class II *E. coli* enzyme did not exhibit this activity (*27*). Using Mg^{2+} as a productive metal ion, the effect of the metal ion on the ability of the *S. shibatae* enzyme to bind to the Val-34C substrate was examined. The concentration of Mg^{2+} was chosen at 2 mM, where the *S. shibatae* enzyme had the maximum activity based on a titration study (data not shown). The *S. shibatae* enzyme was incubated with Val-34C (^{32}P-labeled), with and without the metal ion (2 mM), and its mobility shift was tested on a native gel. Although the gel shift buffer was different from that of the activity assay buffer, the *S. shibatae* enzyme was active in the gel shift condition (data not shown). To ensure that the mobility shift reflected complex formation prior to gel analysis, the gel matrix contained no metal ion. Mobility shift was observed in both conditions, and the extent of the shift was quantitatively similar (Figure 4A), indicating similar binding affinities with and without the metal ion. Thus, the metal ion is not required for the *S. shibatae* enzyme to bind the RNA substrate under the gel shift condition, where a

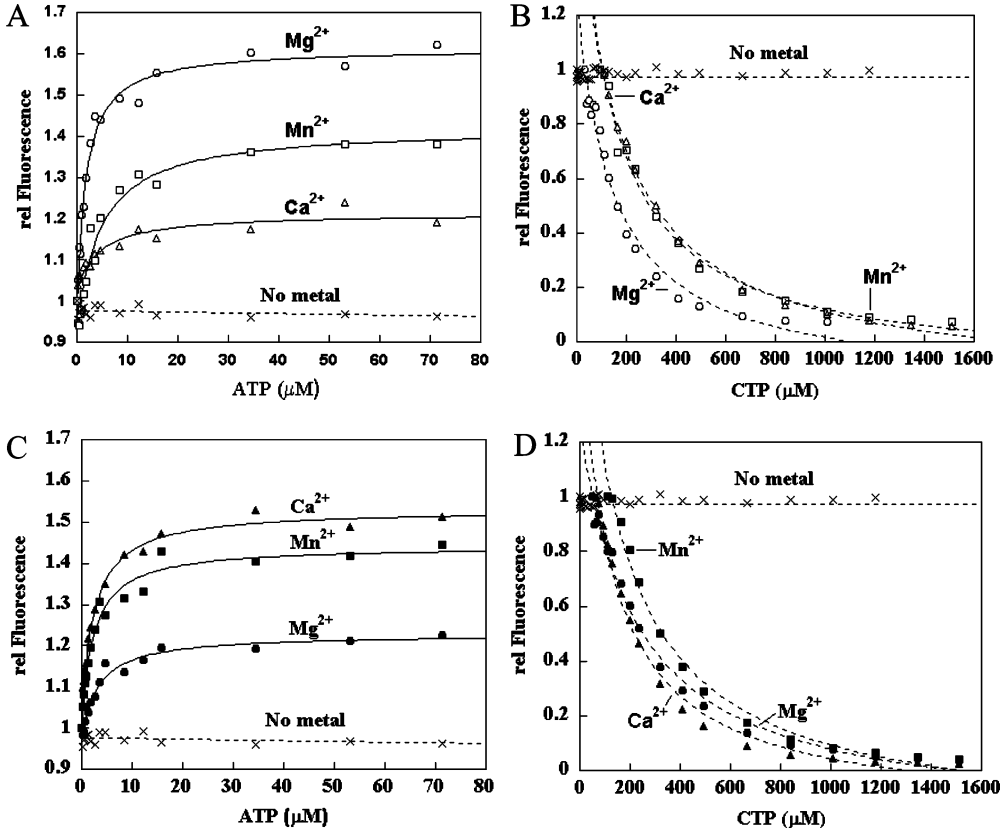

FIGURE 3: Fluorescence titration of binding of ATP or CTP to the *E. coli* (0.5 μM, A, B) and *S. shibatae* (0.5 μM, C, D) enzymes in the presence of 10 mM Mg^{2+}, Mn^{2+}, and Ca^{2+}, or no metal ions. The fluorescence spectrum of ATP titration (A, C) and CTP titration (B, D) was obtained by excitation at 285 nm and monitored of emission at 340 nm for the *E. coli* enzyme, but was monitored of emission at 335 nm for the *S. shibatae* enzyme.

Table 1: Equilibrium Dissociation Constants (μM) Determined by Fluorescence

ligands	Mg^{2+}	Mn^{2+}	Ca^{2+}
E. coli			
ATP	1.8 ± 0.2	4.7 ± 1.2	4.6 ± 1.5
CTP	150 ± 30	130 ± 30	180 ± 20
S. shibatae			
ATP	3.5 ± 0.7	2.5 ± 0.4	2.5 ± 0.3
CTP	230 ± 30	160 ± 40	130 ± 20

large excess of enzyme was used over the RNA substrate. The role of the metal ion in the activity assay, where catalytic amounts of enzyme were used, could not be directly assessed.

Metal Ions Are Responsible for Catalysis. To address the role of metal ions in catalysis, the activity of A76 addition was monitored in the presence of increasing concentrations of Mg^{2+}. The activity of the *E. coli* enzyme showed a steady increase with increasing Mg^{2+} (0.25−1.0 mM) until it reached a plateau around 1 mM (Figure 4B). The same increase of activity was observed for the *S. shibatae* enzyme, although the plateau was reached at 2 mM Mg^{2+} (data not shown). This increase of activity with metal ion concentrations suggested a metal-ion-dependent catalytic mechanism, and the lowest optimal concentration of metal ions at 1−2 mM was consistent with values reported for other enzymes dependent on metal ions for catalysis (*28*).

Assays in the presence of two different metal ions were performed to gain insights into the possibility of a two-metal-ion mechanism. We chose Mg^{2+} as the productive metal ion and Ca^{2+} as the nonproductive ion. If the larger Ca^{2+} was excluded from the Mg^{2+}-binding site, then no effect of increase or decrease on activity should be observed. However, if the activity were dependent on only one metal ion, addition of Ca^{2+} to the Mg^{2+}-binding site should decrease activity. Conversely, if the activity were dependent on two metal ions, which performed different functions (activation of the nucleophilicity of the 3′-OH or stabilization of leaving groups), Ca^{2+} might be better suited for one function than the other so that its presence might enhance the overall activity. Such a synergistic enhancement effect had been reported for several two-metal-ion enzymes (see Discussion). For the *E. coli* enzyme, indeed, the presence of a suboptimal concentration of Ca^{2+} (1 μM) had a small inhibitory effect on the Mg^{2+}-dependent activity, but a significant enhancement effect as Mg^{2+} approached saturation (Figure 4B). The ability of Ca^{2+} to exert effects indicated binding of Ca^{2+} to the enzyme, and the complex behaviors of Ca^{2+} were consistent with two metal sites. In this scenario, Ca^{2+} would be readily accepted by one site, but it must compete with Mg^{2+} at the second site. The small inhibitory effect of Ca^{2+} at low Mg^{2+} concentrations could reflect competition between Ca^{2+} and Mg^{2+} at the second site. As concentrations of Mg^{2+} increased, it fully occupied the second site and worked synergistically with Ca^{2+} at the first to facilitate catalysis.

The *S. shibatae* enzyme also showed an enhancement of activity in the presence of Ca^{2+} (1 μM) above the activities observed with Mg^{2+} alone, although the effect was much smaller (data not shown). To further test the effect of Ca^{2+}, assays were performed using the more active metal ion Mn^{2+} (1 mM) and in the presence of increasing concentrations of

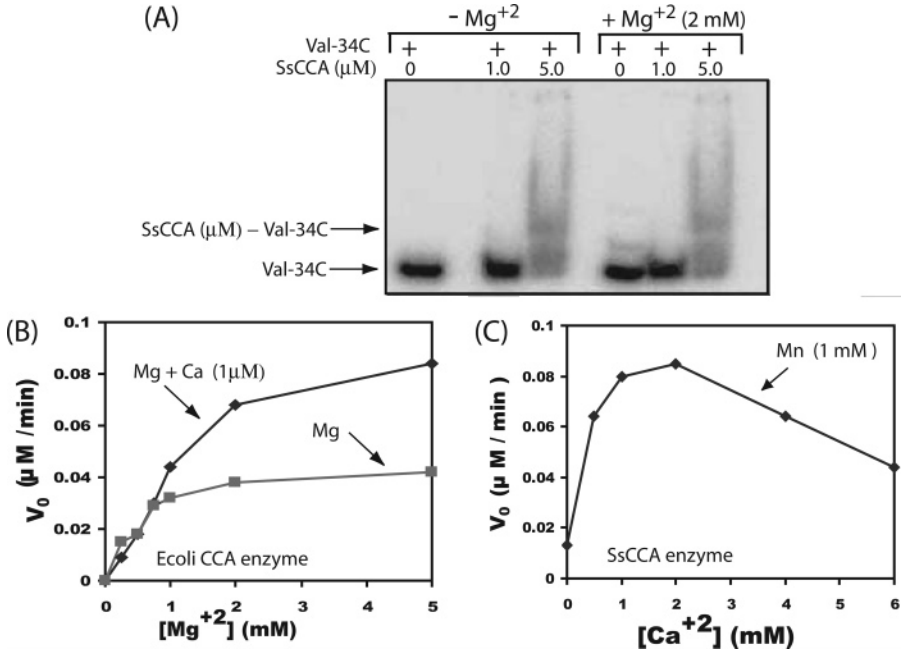

FIGURE 4: (A) Gel shift analysis of the *S. shibate* enzyme binding to the ^{32}P-labeled Val-34C substrate. The RNA (<0.1 μM) was incubated with different concentrations (0, 1.0, 5.0 μM) of the enzyme with and without 2 mM $MgCl_2$. (B) Addition of ATP (250 μM) to Val-34C (1 μM) catalyzed by the *E. coli* enzyme (0.03 μM) in the presence of increasing concentrations of Mg^{2+} (0−5 mM), with or without the coexistence of Ca^{2+} (1 μM). (C) Addition of ATP (250 μM) to Val-34C (1 μM) catalyzed by the *S. shibatae* enzyme (3 μM) in the presence of Mn^{2+} (1 mM) and increasing concentrations of Ca^{2+} (0−6 mM).

Ca^{2+} up to 6 mM (Figure 4C). The Mn^{2+}-dependent activity initially increased with increasing concentrations of Ca^{2+} up to 2 mM, but progressively decreased with further increases of Ca^{2+}. The dual response of activity to Ca^{2+} was also consistent with the two-metal-ion model, where Ca^{2+} at lower concentrations displaced Mn^{2+} from one site to provide a stimulatory effect, and then at higher concentrations, displaced Mn^{2+} from the second site. Because the enzyme with Ca^{2+} at both sites would be inactive, the rise of this species as Ca^{2+} concentrations increased explained the decrease of activity.

Metal Ions for Synthesis of the Noncognate CCC and Poly(C). To determine the role of metal ions in the specificity of nucleotide addition, synthesis of the noncognate CCC and poly(C) by CCA enzymes was investigated (Figure 5A). The Val-34C substrate (^{32}P-labeled) was incubated with CTP, without ATP, so that the synthesis of CCC could be interpreted directly. For both *E. coli* and *S. shibatae* enzymes, the propensity of adding multiple Cs was evident (Figure 5B,C). As such, the rate of conversion was calculated from the decrease of the Val-34C substrate over a time course. Notably, several metal ions supported the *E. coli* enzyme to catalyze the noncognate reaction, with relative activities in an order that is identical to that of the cognate reaction ($Mn^{2+} > Mg^{2+} \gg Zn^{2+} = Co^{2+} \gg Ca^{2+} = Ni^{2+}$) (Figure 2B). In particular, both Mn^{2+} and Mg^{2+} promoted synthesis of CCC, and poly(C), which extended as far as 10 nucleotides in the Mn^{2+} reaction. In contrast, only Mn^{2+} supported the *S. shibatae* enzyme to synthesize CCC and poly(C) (Figure 5C).

Discrimination of Cognate and Noncognate Reactions by Metal Ions. To evaluate how metal ions determine the specificity of nucleotide addition, the kinetics of addition was analyzed for the two productive metal ions Mg^{2+} and Mn^{2+} (Table 2). The *E. coli* enzyme was chosen for this detail kinetic analysis, because it was more versatile, capable of synthesizing the noncognate CCC using both metal ions, whereas the *S. shiabatae* enzyme was limited to only using Mn^{2+} for synthesis of CCC (Figure 5). The flexibility of the *E. coli* enzyme thus allowed analysis of the effect of the two metal ions on both the cognate and noncognate reactions. The results of the *E. coli* enzyme however should be applicable to the *S. shibatae* enzyme, because both display higher activity by Mn^{2+} than by Mg^{2+} (Figure 2), but more specificity by Mg^{2+} than by Mn^{2+} (Figure 5). The kinetic analysis was to compare how the two metal ions affect the K_m and k_{cat} parameters for addition of A76 (cognate) and C76 (noncognate) to the CC end. The reaction conditions here were similar to those described above, except that concentrations of ATP and CTP were varying, rather than saturating (250 μM for ATP in Figure 2, and 250 μM for CTP in Figure 5), to develop a series of velocities in steady-state kinetic conditions (where the enzyme concentrations were ~20-fold below the lowest concentrations of nucleotides). The relationships of velocities and concentrations were then fit to the Michaelis−Menten equation to derive the K_m and V_{max} parameters, and the value of V_{max} was then divided by the enzyme concentration to obtain k_{cat}. Notably, the calculation of k_{cat} was based on the assumption that 100% enzyme was active. The determination of the active fraction of the enzyme must await development of an active-site burst assay for the CCA enzyme. The K_m and the calculated k_{cat} parameters for ATP and CTP are summarized in Table 2.

In the Mg^{2+}-dependent cognate reaction, the K_m for ATP was 3.0 μM, which is closely similar to the K_d determined by the fluorescence assay (1.8 μM, Table 1). The k_{cat} of the reaction was 2.2 min^{-1}, and the overall k_{cat}/K_m was 0.7 μM^{-1} min^{-1}, which were similar to previously determined values (*21*). In the noncognate reaction, the K_m for CTP was 150 μM, which is identical to the K_d determined by the fluorescence assay (150 μM, Table 1). The k_{cat} of the

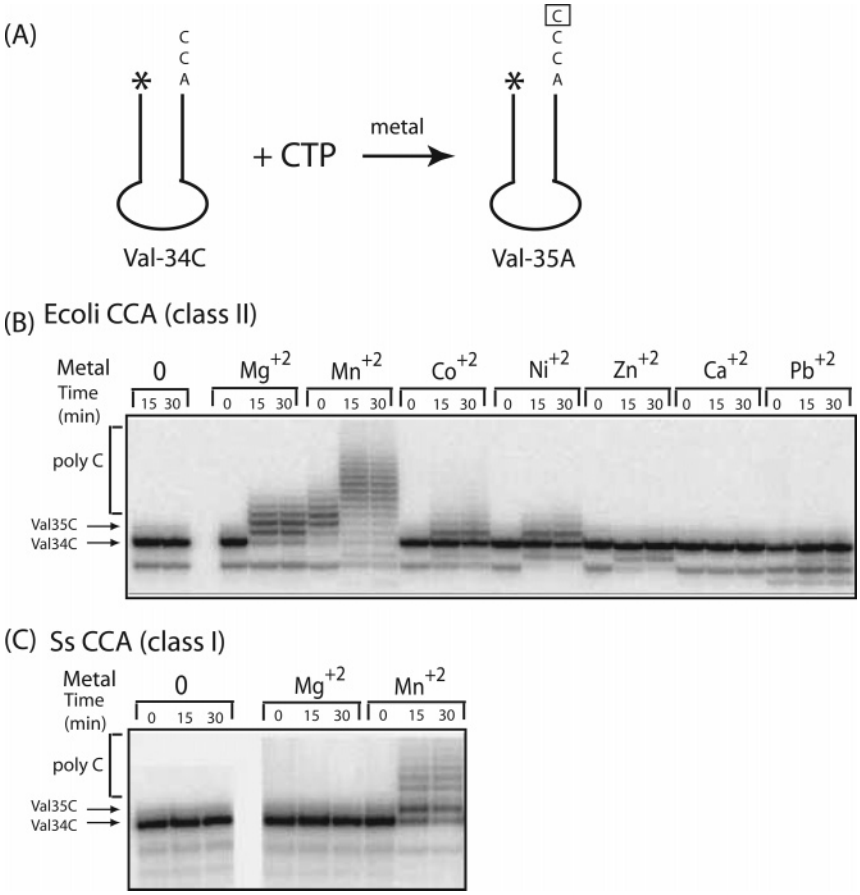

FIGURE 5: (A) Addition of CTP (250 μM) to Val-34C (1 μM, 5′ labeled) catalyzed by a CCA enzyme in the presence of different divalent metal ions (1 mM each). (B) Addition catalyzed by the class II *E. coli* enzyme (0.02 μM). (C) Addition catalyzed by the class I *S. shibate* enzyme (17 μM). The time course of the metal-dependent reactions is shown for each metal ion, and the positions of Val-34C and Val-35C are indicated by arrows.

Table 2: Kinetic Parameters of Nucleotide Addition to Position 76 by the *E. Coli* CCA Enzyme[a]

metal	nucleotide	K_m (μM)	k_{cat} (min^{-1})	k_{cat}/K_m (μM^{-1} min^{-1})	specificity factor
Mg^{2+}	ATP	3.0 ± 0.9	2.2 ± 0.4	0.7	1.8×10^3
	CTP	150 ± 20	0.066 ± 0.01	4×10^{-4}	
Mn^{2+}	ATP	3.3 ± 2.0	21.2 ± 2.0	7.5	1.5×10^1
	CTP	4.7 ± 1.3	2.3 ± 0.1	5.1×10^{-1}	

[a] For the Mg^{2+}-dependent cognate reaction, the *E. coli* enzyme (0.03 μM) was incubated with the Val-34C substrate (1 μM) and ATP (0.5−20 μM) for 0−15 min. The noncognate reaction contained the enzyme (0.3 μM), Val-34C (1 μM), and CTP (20−500 μM) for 0−45 min. For the Mn^{2+}-dependent cognate reaction, the *E. coli* enzyme (0.01 μM) was incubated with Val-34C (1 μM) and ATP (0.5−20 μM) for 0−15 min, while the Mn^{2+}-dependent noncognate reaction contained the enzyme (0.01 μM), Val-34C (1 μM), and CTP (0.5−20 μM) for 1−15 min. Each reaction was repeated at least 3 times, and the average was reported with standard errors of deviation.

noncognate reaction, however, was significantly lower (0.066 min^{-1}) relative to that of the cognate reaction. By comparing the catalytic efficiency (k_{cat}/K_m) for synthesis of CCA and CCC, the discrimination factor by the Mg^{2+} ion was about 2000-fold (Table 2).

In the Mn^{2+}-dependent reaction, the K_m for ATP (3.3 μM) in the cognate reaction was essentially the same as that in the Mg^{2+} reaction, but the k_{cat} (21 min^{-1}) was higher by nearly 10-fold. This resulted in an overall greater value of k_{cat}/K_m, confirming that Mn^{2+} promoted a better efficiency than Mg^{2+} for the cognate reaction as shown in Figure 2. In the noncognate reaction, the K_m for CTP was 4.7 μM, which is a 30-fold improvement from the K_m for CTP in the Mg^{2+}-dependent reaction. Additionally, the k_{cat} for the noncognate reaction (2.3 min^{-1}) increased 30-fold from that of the Mg^{2+}-dependent reaction. The changes in both K_m and k_{cat} brought the overall k_{cat}/K_m to 0.5 μM^{-1} min^{-1}, significantly higher than that of the corresponding noncognate reaction by Mg^{2+} (4×10^{-4} μM^{-1} min^{-1}). Thus, Mn^{2+} improved both the cognate and noncognate efficiency, but it had a more pronounced effect on the noncognate reaction. As a result, the discrimination factor by Mn^{2+} was reduced to about 20, suggesting a 100-fold decreased specificity compared to Mg^{2+}.

The Physiologically Relevant Metal Ion. Although Mg^{2+} promoted specificity while Mn^{2+} decreased specificity, the physiological relevance of these two metal ions needed to be established in a condition where ATP and CTP are both present. Such a condition challenged the CCA enzymes to select ATP to add to the CC end. To determine the physiological relevance of these metal ions, the addition of nucleotide 76 to Val-34C was determined in the presence

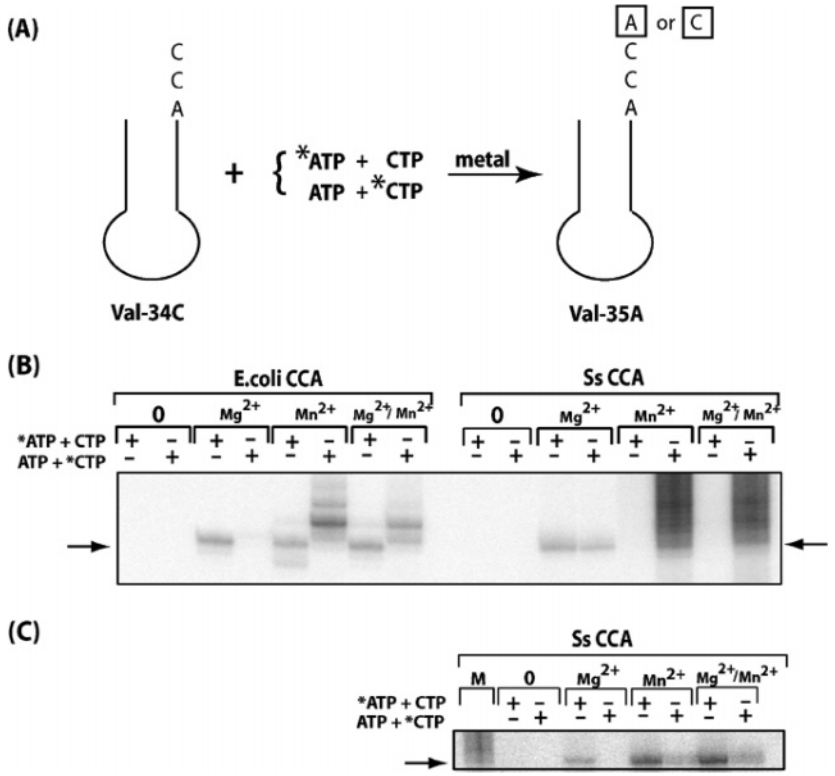

FIGURE 6: (A) Addition to the 76 position of Val-34C catalyzed by the *E. coli* (0.03 μM, 37 °C) or *S. shibatae* (1.5 μM, 60 °C) CCA enzymes in the presence of 10 mM metal ions and ATP and CTP for 15 min, where either [α-^{32}P]ATP or [α-^{32}P]CTP was added. (B) Addition was performed when ATP and CTP were 250 μM each, where the repetitive pattern of synthesis is marked by a dot next to the beginning of a triplet (presumably CCA). (C) Addition was performed when ATP was at 1 mM and CTP at 50 μM. The arrows indicate the first position of addition, i.e., 76. "M" denotes the marker, which was the poly(C) synthesis obtained from panel B.

of both ATP and CTP. To identify which nucleotide was selected for addition, only one of the nucleotides was labeled (Figure 6A). In this design, if a product was identified in the reaction labeled with ATP, but not in the reaction labeled with CTP, this would suggest addition of A but not C, and vice versa. If a product was detected in the ATP-labeled reaction, and also in the CTP-labeled reaction, this would suggest addition of both A and C to the same position.

With Mg^{2+} at 1 mM, and ATP and CTP each at 250 μM, the *E. coli* enzyme incorporated just one nucleotide, which was A76, because it was labeled by ATP (Figure 6B, lane 2) but not by CTP (lane 3). With Mn^{2+} at 1 mM, however, the *E. coli* enzyme incorporated multiple nucleotides (lanes 4, 5), the pattern of which was quite different from that of a poly(C) ladder generated by the SsCCA enzyme (lanes 12, 14). The first nucleotide (i.e. position 76) was A76, because it was labeled only by ATP (lane 4) but not by CTP (lane 5). The next nucleotide was a C, as labeled by CTP (lane 5) but not by ATP (lane 4). This was then followed by a spacing of two nucleotides, which were interpreted from the labeled CTP reaction (lane 5) as a weakly labeled C and an unlabeled A. The intermittent pattern was also observed in the labeled ATP reaction (lane 4), but only weakly, due to the dominant labeling of A76. Because the intermittent pattern was observed only when ATP was mixed with CTP, but not when CTP was used as the sole substrate (as in Figure 5B), the most likely interpretation for the multiple nucleotides was polymers of CCA, although the possibility of poly(C) could not be completely excluded. The intermittent pattern was also detectable when the *E. coli* enzyme was tested in the presence of both Mg^{2+} and Mn^{2+}. Because Mg^{2+} catalyzed synthesis of just one CCA, whereas Mn^{2+} catalyzed synthesis of polymers, Mg^{2+} is the physiological relevant metal ion.

The unexpected synthesis of polymers by the *E. coli* enzyme with Mn^{2+} prompted analysis of the activity of the *S. shibatae* enzyme in the presence of Mn^{2+} first, with ATP and CTP each at 250 μM (lanes 11, 12). Instead of synthesizing CCA or polymers of CCA, this enzyme synthesized only a ladder of poly(C) (lane 12), without evidence of incorporation of A (lane 11). The robust poly(C) synthesis remained active, with addition of Mg^{2+} to the Mn^{2+} reaction (lanes 13, 14). Differences from the *E. coli* enzyme were also found in the Mg^{2+}-catalyzed reaction. Although the *S. shibatae* enzyme used Mg^{2+} to catalyze addition of just one nucleotide, this nucleotide was largely C (lane 10), with only a small fraction being A (lane 9), suggesting that CCC was the major product. Thus, under the experimental condition, the *S. shibatae* enzyme was unable to synthesize CCA with either Mg^{2+} or Mn^{2+}.

Experimental conditions were then modified to concentrations of ATP (1 mM) and CTP (50 μM) more akin to those of physiological conditions (Figure 6C). Here, Mg^{2+} promoted synthesis of CCA, because there was addition of just one nucleotide, which was labeled only by ATP (lane 17), but not by CTP (lane 18). In contrast, Mn^{2+} promoted addition of A (lane 19), as well as C (lane 20). Upon a prolonged exposure, incorporation of multiple Cs was also detected (lane 20). When Mg^{2+} and Mn^{2+} were both present, the phenotype of Mn^{2+} dominated (lane 22). These results demonstrated that, at physiological nucleotide concentrations, Mg^{2+} ensured the specificity of CCA and thus is the biologically relevant metal ion for the *S. shibatae* enzyme.

DISCUSSION

Metal Ions Catalysis. This study provides functional support to the structural prediction that members of class I and class II CCA enzymes, as exemplified by the *S. shibatae* and *E. coli* enzymes, respectively, use metal ions for catalysis. This functional confirmation is an important step forward to understand the catalytic mechanism of CCA enzymes, and to relate them to DNA and RNA polymerases. We show here that the activity of both the *E. coli* and *S. shibatae* CCA enzymes is strictly dependent on metal ions, that the activity is highest with Mg^{2+} or Mn^{2+} as the cofactor, but nondetectable with Ca^{2+} as the cofactor, and that the activity increases with increasing concentrations of Mg^{2+} up to a maximum at about 1−2 mM (Figure 4A). In addition, although metal ions are not required for binding of the RNA substrate, at least in the case of the *S. shibatae* enzyme (Figure 4A), they are necessary for binding of ATP and CTP for both enzymes (Figure 3). The role of metal ions in nucleotide binding may be to stabilize and help to shape the structure of the active site. Additionally and alternatively, metal ions may accompany nucleotides for entry into the active site. In a recent crystal structure of the eukaryotic RNA polymerase (pol II), only one metal ion was detected in the apo-enzyme, while a second metal ion was found to be coordinated by the β and γ phosphates of the incoming nucleotide (*29*). The geometry of the second metal was in a similar spatial relationship with the enzyme-bound metal and nucleotide as those reported for DNA and RNA polymerases that use the two-metal-ion mechanism. This provides evidence that even for enzymes known to use the two-metal-ion mechanism, such as pol II, one of the two metal ions is required to bind the nucleotide substrate in order to enter the active site to participate in catalysis.

Although this study provides clear evidence that metal ions are responsible for catalysis, the experiments here do not definitively prove that two metal ions are involved in catalysis. For example, in the mixing experiments of two different metal ions, alternative explanations could be proposed for the enhancement effect of Ca^{2+} to the *E. coli* enzyme (Figure 4B), such as the possibility that Ca^{2+} might function strictly to stabilize nucleotide binding but not catalysis. Similarly, the enhancement effect of low concentrations of Ca^{2+} to the *S. shibatae* enzyme (Figure 4C) could be due to the ability of Ca^{2+} to displace Mn^{2+} from other bound states in the assay (such as the nucleotide or RNA substrate), so that Ca^{2+} actually enhances the binding of Mn^{2+} to the active site. However, these alternative models do not sufficiently address why the effect of Ca^{2+} at low Mg^{2+} concentrations on the *E. coli* enzyme is inhibitory (Figure 4B), and why higher concentrations of Ca^{2+} decrease the *S. shibatae* enzyme activity (Figure 4C). The complex effect of a nonproductive metal ion, such as Ca^{2+} here, has been observed previously for other two-metal-ion enzymes. For example, Ca^{2+} at low concentrations (<2 mM) stimulates the activity of the restriction enzyme *Eco*RV, but at higher concentrations it inhibits the enzyme activity (*30*). In the human apurinic/apyrimidinic endonuclease, *Ape*I, Ca^{2+} stimulates the activity at low concentrations of Mg^{2+}, but inhibits activity at higher concentrations of Mg^{2+} (*31*). In other examples, even the combination of two productive metal ions together can have a complex effect. For example, the Mg^{2+}-dependent activity of the influenza virus endonuclase is stimulated by low concentrations of Mn^{2+}, but the stimulatory effect is small at low concentrations of Mg^{2+} (0.001−0.1 mM), larger at higher concentrations of Mg^{2+} (0.1−1.0 mM), then becomes smaller again as Mg^{2+} concentrations increase (*28*). Similar effects have been reported for the hammerhead ribozyme, where a synergistic enhancement of activity is observed by a combination of La^{3+} and Mg^{2+} (*32*), and for the lead-zyme by a combination of Pb^{2+} and Nd^{3+} (*33*). These precedents suggest that the complex behaviors of Ca^{2+} on the *E. coli* and *S. shibatae* enzymes are most consistent with a two-metal-ion mechanism. Also, the presence of the DXD motif in CCA enzymes also agrees with other two-metal-ion enzymes, whereas enzymes that use only one metal ion for catalysis lack the DXD motif and require an additional catalytic residue, usually a histidine (*34*). However, it should still be recognized that additional biochemical and structural determinations must be performed to unequivocally prove the two-metal-ion mechanism for CCA synthesis.

Metal-Ion-Dependent Specificity. This study also clearly demonstrates that metal ions have a direct role in CCA enzymes for determining the specificity of nucleotide incorporation. The reaction catalyzed by both the *E. coli* and *S. shibatae* enzymes in the presence of the Mg^{2+} cofactor showed higher specificity under the assay conditions as compared to that in the presence of the Mn^{2+} cofactor (Figure 6B,C). In the detailed kinetic analysis of the *E. coli* enzyme (Table 2), the specificity factor of Mg^{2+} is roughly ∼2000, while that of Mn^{2+} is ∼20, so that Mg^{2+} is more specific than Mn^{2+} by 100-fold. The driving force of Mg^{2+}-dependent specificity is a lower K_m for ATP than for CTP (50-fold) and a higher k_{cat} (30−40-fold). When Mn^{2+} is used for catalysis, however, the K_m effect is abolished, while the k_{cat} effect is reduced to 10-fold against the noncognate reaction. Overall, the reduced specificity by Mn^{2+} is due to a nearly 10^3-fold improvement for the noncognate reaction, but only a 10-fold improvement for the cognate reaction.

The relaxed specificity by Mn^{2+} due to the preferential promotion of the noncognate reaction over the cognate reaction is rare among enzymes that use metal ion catalysis. In most cases, the decrease of specificity by Mn^{2+} is attributed to an increase of the rate of the noncognate reaction, as is seen here, but also to a decrease of the rate of the cognate reaction. This has been shown for several restriction enzymes, including *Eco*RV (*15*), *Eco*RI (*16*), and *Taq*I (*35*). Because Mn^{2+} is a stronger Lewis acid (lowering more pK_a of an associated water molecule) than Mg^{2+}, and has a higher intrinsic affinity to the phosphate oxygens of the nucleic acid backbone, this metal ion is likely to promote a higher rate of the chemistry step. In fact, more detailed kinetic analysis of *Eco*RV and *Taq*I has confirmed that Mn^{2+} indeed enhances the rate of the chemistry step of both cognate and noncognate reactions, but that it inhibits the rate of product release for the cognate reaction, resulting in the overall reduced rate of the cognate reaction (*15*, *35*, *36*).

New insights into the kinetic mechanism of CCA enzymes are obtained from comparison of the K_d and K_m values for ATP and CTP (Tables 1, 2). With Mg^{2+} as the cofactor, the *E. coli* enzyme exhibits K_d and K_m for ATP (1.8, 3.0 μM) closely similar to each other. The same is true for K_d and K_m for CTP (150 μM). In steady-state kinetics, when $K_d \sim K_m$, the rate-limiting step is enzyme turnover (k_{cat}). Specif-

ically, $K_m = (k_{-1}/k_1) + (k_{cat}/k_1)$, where k_1 and k_{-1} are the association and dissociation rates of a substrate binding to the enzyme, respectively. When K_m is approaching K_d, which is defined by k_{-1}/k_1, the factor k_{cat}/k_1 must be negligible. This requires that k_{cat} be small as compared to k_1, such that enzyme turnover becomes the rate-limiting step. In contrast, with Mn^{2+} as the cofactor, while parameters for ATP remain little changed, those for the noncognate CTP have changed, primarily by reducing the K_m for CTP to a level (4.7 μM) that it is significantly smaller than K_d (160 μM). This raises the possibility that, in the noncognate reaction, Mn^{2+} may have altered the reaction profile, such that k_{cat} has been accelerated to the point that it is no longer rate limiting. Thus, metal ions have the ability to alter the rate-limiting step in the reaction pathway, providing a major determinant for the specificity of CCA synthesis.

Differences between the Two Classes. This study has revealed subtle differences between the *E. coli* and *S. shibatae* CCA enzymes. Of most interest was the observation that, in the experiments of mixing metal ions, the *E. coli* enzyme has a higher sensitivity to Ca^{2+} and responds to μM concentrations of the nonproductive metal ion, whereas the *S. shibatae* enzyme responds to mM concentrations (Figure 4B,C). The *E. coli* enzyme also accommodates a wider range of metal ions for activation (Mg^{2+}, Mn^{2+}, Co^{2+}, Ni^{2+}, and Zn^{2+}), whereas the *S. shibatae* enzyme is limited to only Mg^{2+} and Mn^{2+}. The broader metal specificity of the *E. coli* enzyme suggests more flexibility in metal coordination sphere and is consistent with its ability to better respond to Ca^{2+}.

The *E. coli* and *S. shibatae* enzymes also differ in their ability to select ATP in challenging conditions, where both ATP and CTP are present. Although both enzymes use Mg^{2+} as the physiological metal ion, the *E. coli* enzyme readily selects ATP against CTP at 250 μM each. In contrast, the *S. shibatae* enzyme achieves the specificity only under the more physiologically relevant conditions, where ATP is at 1 mM and CTP at 50 μM. Because there is only one active site in both classes of CCA enzymes, this single active site must change the specificity between ATP and CTP depending on cellular concentrations of nucleotides and on the sequence of the tRNA 3′ end. The more stringent requirement of the *S. shibatae* enzyme suggests a more rigid active site, consistent with its more restricted ability to bind different metal ions.

Perhaps the most interesting and unexpected difference is the effect of Mn^{2+} on the selectivity of ATP under challenging conditions. While Mn^{2+} decreases the specificity of both enzymes, the outcome is quite different. In our analysis of Figure 6, Mn^{2+} appears to enable the *E. coli* enzyme to synthesize polymers of CCA under challenging conditions. Although additional experiments are needed to confirm poly(CCA) synthesis, this activity would suggest that the ordered synthesis of CCA is maintained but that the constraint of synthesizing just one CCA is lost. The poly(CCA) activity has not been reported for the wild-type *E. coli* enzyme before, but has recently been shown for a variant that has swapped a C-terminal region of 27 amino acids with the analogous region of the poly(A) polymerase (*37*). It is proposed that the region of the 27 amino acids is an anchor of the *E. coli* CCA enzyme that restricts polymerization to just three nucleotides. Here, Mn^{2+} might have the ability to eliminate the anchor effect on the wild-type *E. coli* enzyme, mimicking the behavior of the C-terminally altered mutant. In contrast, the effect of Mn^{2+} in *S. shibatae* enzyme is solely to promote the poly(C) synthesis, which suggests that incorporation of C is so fast that it completely suppresses incorporation of A.

Whether the differences between the *E. coli* and *S. shibatae* enzymes represent differences of the two classes of CCA enzymes is not known. However, the requirement of mM concentrations of ATP for the class I *S. shibatae* enzyme specificity has been reported previously for the class I enzyme of *Methanococcus jannaschii* (*21*), suggesting the possibility that this feature might be common to all class I enzymes. Further analysis of other members of each class is necessary to derive a more definitive conclusion, and may reveal additional differences between the two classes. Consistent with this, functional analysis has already identified another key difference between the two classes: while all three conserved carboxylates in the active site are required for class I activity, only the two of the DXD motif are required for class II activity (*6*). This example, together with differences identified here between the *E. coli* and *S. shibatae* enzymes, further emphasize the divergent evolution of the two classes, even up to details of the conserved catalytic core. Importantly, despite the extensive divergence, the two classes of CCA enzymes have preserved a common catalysis mechanism that uses divalent metal ions to determine specificity.

ACKNOWLEDGMENT

We thank Svetlana Shtivelband and Amanda Roberts for assistance and discussion, and Dr. Howard Gamper for critical reading of the manuscript.

REFERENCES

1. Deutscher, M. P. (1982) tRNA nucleotidyltransferase, *Enzymes 15*, 183−215.
2. Maizels, N., and Weiner, A. M. (1994) Phylogeny from function: evidence from the molecular fossil record that tRNA originated in replication, not translation, *Proc. Natl. Acad. Sci. U.S.A. 91*, 6729−34.
3. Li, F., Xiong, Y., Wang, J., Cho, H. D., Tomita, K., Weiner, A. M., and Steitz, T. A. (2002) Crystal structures of the Bacillus stearothermophilus CCA-adding enzyme and its complexes with ATP or CTP, *Cell 111*, 815−24.
4. Okabe, M., Tomita, K., Ishitani, R., Ishii, R., Takeuchi, N., Arisaka, F., Nureki, O., and Yokoyama, S. (2003) Divergent evolutions of trinucleotide polymerization revealed by an archaeal CCA-adding enzyme structure, *EMBO J. 22*, 5918−27.
5. Xiong, Y., Li, F., Wang, J., Weiner, A. M., and Steitz, T. A. (2003) Crystal structures of an archaeal class I CCA-adding enzyme and its nucleotide complexes, *Mol. Cell 12*, 1165−72.
6. Augustin, M. A., Reichert, A. S., Betat, H., Huber, R., Morl, M., and Steegborn, C. (2003) Crystal Structure of the Human CCA-adding Enzyme: Insights into Template-independent Polymerization, *J. Mol. Biol. 328*, 985−94.
7. Xiong, Y., and Steitz, T. A. (2004) Mechanism of transfer RNA maturation by CCA-adding enzyme without using an oligonucleotide template, *Nature 430*, 640−5.
8. Tomita, K., Fukai, S., Ishitani, R., Ueda, T., Takeuchi, N., Vassylyev, D. G., and Nureki, O. (2004) Structural basis for template-independent RNA polymerization, *Nature 430*, 700−4.
9. Yue, D., Weiner, A. M., and Maizels, N. (1998) The CCA-adding enzyme has a single active site, *J. Biol. Chem. 273*, 29693−700.
10. Steitz, T. A., and Steitz, J. A. (1993) A general two-metal-ion mechanism for catalytic RNA, *Proc. Natl. Acad. Sci. U.S.A. 90*, 6498−502.

11. Steitz, T. A. (1998) A mechanism for all polymerases [news; comment], *Nature 391*, 231−2.
12. Pelletier, H., Sawaya, M. R., Kumar, A., Wilson, S. H., and Kraut, J. (1994) Structures of ternary complexes of rat DNA polymerase beta, a DNA template-primer, and ddCTP, *Science 264*, 1891−903.
13. Martin, G., Keller, W., and Doublie, S. (2000) Crystal structure of mammalian poly(A) polymerase in complex with an analog of ATP [In Process Citation], *EMBO J. 19*, 4193−203.
14. Fedor, M. J. (2002) The role of metal ions in RNA catalysis, *Curr. Opin. Struct. Biol. 12*, 289−95.
15. Vermote, C. L., Vipond, I. B., and Halford, S. E. (1992) EcoRV restriction endonuclease: communication between DNA recognition and catalysis, *Biochemistry 31*, 6089−97.
16. Hsu, M., and Berg, P. (1978) Altering the specificity of restriction endonuclease: effect of replacing Mg2+ with Mn2+, *Biochemistry 17*, 131−38.
17. Lagunavicius, A., Grazulis, S., Balciunaite, E., Vainius, D., and Siksnys, V. (1997) DNA binding specificity of MunI restriction endonuclease is controlled by pH and calcium ions: involvement of active site carboxylate residues, *Biochemistry 36*, 11093−9.
18. Jeltsch, A., Alves, J., Wolfes, H., Maass, G., and Pingoud, A. (1994) Pausing of the restriction endonuclease EcoRI during linear diffusion on DNA, *Biochemistry 33*, 10215−9.
19. Tabor, S., and Richardson, C. C. (1989) Effect of manganese ions on the incorporation of dideoxynucleotides by bacteriophage T7 DNA polymerase and Escherichia coli DNA polymerase I, *Proc. Natl. Acad. Sci. U.S.A. 86*, 4076−80.
20. Hou, Y. M. (2000) Unusual synthesis by the Escherichia coli CCA-adding enzyme [In Process Citation], *RNA 6*, 1031−43.
21. Seth, M., Thurlow, D. L., and Hou, Y. M. (2002) Poly(C) synthesis by class I and class II CCA-adding enzymes, *Biochemistry 41*, 4521−32.
22. Arthur, P. G., and Hochachka, P. W. (1995) Automated analysis of cellular metabolites at nanomolar to micromolar concentrations using bioluminescent methods, *Anal. Biochem. 227*, 281−4.
23. Turnbough, C. L., Jr. (1983) Regulation of Escherichia coli aspartate transcarbamylase synthesis by guanosine tetraphosphate and pyrimidine ribonucleoside triphosphates, *J. Bacteriol. 153*, 998−1007.
24. Shi, P. Y., Weiner, A. M., and Maizels, N. (1998) A top-half tDNA minihelix is a good substrate for the eubacterial CCA- adding enzyme, *RNA 4*, 276−84.
25. Hegg, L. A., Kou, M., and Thurlow, D. L. (1990) Recognition of the tRNA-like structure in tobacco mosaic viral RNA by ATP/CTP: tRNA nucleotidyltransferases from Escherichia coli and Saccharomyces cerevisiae, *J. Biol. Chem. 265*, 17441−5.
26. Tomari, Y., Suzuki, T., Watanabe, K., and Ueda, T. (2000) The role of tightly bound ATP in Escherichia coli tRNA nucleotidyltransferase, *Genes Cells 5*, 689−98.
27. Shi, P. Y., Maizels, N., and Weiner, A. M. (1998) CCA addition by tRNA nucleotidyltransferase: polymerization without translocation?, *EMBO J. 17*, 3197−206.
28. Doan, L., Handa, B., Roberts, N. A., and Klumpp, K. (1999) Metal ion catalysis of RNA cleavage by the influenza virus endonuclease, *Biochemistry 38*, 5612−9.
29. Westover, K. D., Bushnell, D. A., and Kornberg, R. D. (2004) Structural basis of transcription: nucleotide selection by rotation in the RNA polymerase II active center, *Cell 119*, 481−9.
30. Vipond, I. B., Baldwin, G. S., and Halford, S. E. (1995) Divalent metal ions at the active sites of the EcoRV and EcoRI restriction endonucleases, *Biochemistry 34*, 697−704.
31. Beernink, P. T., Segelke, B. W., Hadi, M. Z., Erzberger, J. P., Wilson, D. M., 3rd, and Rupp, B. (2001) Two divalent metal ions in the active site of a new crystal form of human apurinic/apyrimidinic endonuclease, Ape1: implications for the catalytic mechanism, *J. Mol. Biol. 307*, 1023−34.
32. Lott, W. B., Pontius, B. W., and von Hippel, P. H. (1998) A two-metal ion mechanism operates in the hammerhead ribozyme-mediated cleavage of an RNA substrate, *Proc. Natl. Acad. Sci. U.S.A. 95*, 542−7.
33. Ohmichi, T., and Sugimoto, N. (1997) Role of Nd3+ and Pb2+ on the RNA cleavage reaction by a small ribozyme, *Biochemistry 36*, 3514−21.
34. Shen, Y., Zhukovskaya, N. L., Guo, Q., Florian, J., and Tang, W. J. (2005) Calcium-independent calmodulin binding and two-metal-ion catalytic mechanism of anthrax edema factor, *EMBO J. 24*, 929−41.
35. Cao, W., Mayer, A. N., and Barany, F. (1995) Stringent and relaxed specificities of TaqI endonuclease: interactions with metal cofactors and DNA sequences, *Biochemistry 34*, 2276−83.
36. Sam, M. D., and Perona, J. J. (1999) Catalytic roles of divalent metal ions in phosphoryl transfer by EcoRV endonuclease, *Biochemistry 38*, 6576−86.
37. Betat, H., Rammelt, C., Martin, G., and Morl, M. (2004) Exchange of regions between bacterial poly(A) polymerase and the CCA-adding enzyme generates altered specificities, *Mol. Cell 15*, 389−98.

BI0509402